ceramics

MDPI

Article

Porous Alumina-Bentonite Ceramics: Effects of Fillers and Molding Technique

Aleksey D. Smirnov [1], Anastasia A. Kholodkova [2,*], Viktor V. Rybalchenko [3] and Vadim P. Tarasovskii [3]

[1] Center of Collective Usage "High-Tech Chemical Technologies", Moscow Polytechnical University, 107023 Moscow, Russia
[2] Chemistry Department, M.V. Lomonosov Moscow State University, 119991 Moscow, Russia
[3] Mobile Solutions Engineering Center, MIREA-Russian Technological University, 119454 Moscow, Russia
* Correspondence: anastasia.kholodkoval@gmail.com

Abstract: In porous ceramics processing, the green body shaping technique largely determines the control of the final porous structure and material properties. The study is aimed at finding affordable approaches for the shaping of two different narrow-fraction fillers: F240 electro-corundum and hollow alumina microspheres. The results revealed the influence of accessible shaping techniques (semi-dry pressing, direct casting, and slip casting) on the structural and mechanical properties of porous alumina ceramics. The starting materials were characterized by XRD, SEM, EDX, and BET. The manufactured ceramics were studied in terms of microstructure, density, porosity, and flexural strength. Free stacking of the fillers' particles during the direct and slip casting resulted in a higher porosity of ceramics compared with that of semi-dry pressing, while reducing its mechanical strength. Direct casting appeared preferable for ceramics with hollow microspheres because it maintained the integrity of the filler particles and preserved their inherent porosity in the ceramics. The optimal parameters for porous ceramics processing were determined as follows: pressing at 30 MPa and sintering at 1280–1320 °C with a bentonite content of 15 wt.%. In this case, the average density and open porosity of F240 samples reached 2.22 g cm^{-3} and 40.4%, while samples containing hollow microspheres reached 2.20 g cm^{-3} and 36.7%, respectively.

Keywords: porous alumina ceramics; electrocorundum; hollow alumina microspheres; pressing; direct casting; slip casting

Citation: Smirnov, A.D.; Kholodkova, A.A.; Rybalchenko, V.V.; Tarasovskii, V.P. Porous Alumina-Bentonite Ceramics: Effects of Fillers and Molding Technique. *Ceramics* **2023**, *6*, 132–145. https://doi.org/10.3390/ceramics6010009

Academic Editor: Angel L. Ortiz

Received: 14 November 2022
Revised: 8 December 2022
Accepted: 4 January 2023
Published: 10 January 2023

1. Introduction

Porous permeable ceramics are widely used in many modern industries such as metallurgy, energy, chemical engineering, food production, medicine, etc. [1,2]. This class of materials serves as filtration elements and separation units, thermal and noise insulators, catalyst carriers, and successfully competes with its metal-, glass-, and plastic-based analogs [1,3]. Due to its high strength, chemical and heat resistance, as well as compatibility with biological tissues, a special place among porous ceramic materials is occupied by ceramics manufactured using alumina narrow-fraction fillers [4,5].

Quite a few manufacturing approaches have been developed to achieve the necessary combination of permeability and mechanical strength of porous ceramics, including those with alumina fillers [6]. Among these approaches, traditional ones could be distinguished, such as dry and semi-dry pressing with subsequent sintering [7–10], the use of pore-forming agents [4,11–15], impregnation of polymer spongy materials [16,17], foaming process [18–22], as well as relatively new ones; for example, gel casting [14,23–25], freeze casting [26,27], self-propagating high-temperature synthesis [28–30], and the use of hollow microspheres as a filler [31–37]. The industrialization of any approach is determined by its technological complexity, availability of raw materials, final product quality, and environmental impact [38]. For example, when using pore-forming agents, homogeneous

microporous ceramics appeared difficult to obtain because of insufficient dispersion of the agent in the raw material [4,10]. The burnout of auxiliary polymer components is associated with a significant release of decomposition products and, consequently, with an additional environmental impact [24]. The ceramics prepared by the foaming process is known to achieve low mechanical strength [10].

In the porous Al_2O_3-based ceramics industry, alumina powders are known as the most commonly used filler [7,9–11,13,18,20,23,24], along with boehmite γ-AlOOH [4] and aluminum hydroxide $Al(OH)_3$ [8,19,38]. In addition, there is an increasing interest in hollow alumina microspheres as a filler [31–35,39]. The comparatively high cost of this raw material could be justified by the control of pore types in final ceramics when using different sizes of microspheres and varying the amount of the binder.

Semi-dry pressing is known as one of the most simple, low-cost, and ecologically benign methods of porous ceramics shaping. To obtain items of complex shape, casting techniques [20,40] as well as additive manufacturing techniques [35] could be applied. 3D printing of ceramics, including porous, is a rapidly developing technological branch [41]. However, its industrial realization is often connected to high expenses because of the special equipment required and expensive auxiliary substances. In some cases, choosing a more custom technique to obtain a complex-shaped item might be considered optimum.

A key factor affecting the microstructure of porous ceramics is the stacking of the filler particles during the shaping process [28,42,43]. Thereby, the use of Al_2O_3 with different morphology (isometric and plate-like particles [9,10]), as well as mechanically treated alumina [9], and alumina with different dispersion compositions [44,45] was examined to increase the porosity and the strength of final ceramics. Meanwhile, it should not be overlooked that the filler morphology could be differently manifested in the microstructure of the ceramics, and it is likely to depend substantially on the shaping technique. However, this point is not widely discussed in the literature.

In the current research, three different shaping techniques are demonstrated in the processing of porous alumina ceramics with bentonite binder: (1) uniaxial static semi-dry pressing, (2) direct casting with a paraffin binder, and (3) slip casting. The filler was selected by its chemical inertness (no gas ejection on sintering) and controlled morphology. Electrocorundum and hollow alumina microspheres (HAM) meet these requirements, and the first is known to be effective in ceramics processing with different binders [43,45–48]. Ceramics based on HAM are prepared by the pressing technique most often [31–33]; therefore, there is interest in examining widely available casting techniques in their production. The comparison of the materials prepared from bulk and hollow alumina particles in different shaping approaches would elucidate how the pressure applied during the shaping affects their microstructures and mechanical properties.

2. Materials and Methods

2.1. Materials

Two types of alumina powders were used as starting materials (Figure 1): (1) electrocorundum F240 with a particle size of 10–100 μm (JSC RUSAL Boksitogorsk, Russia) and (2) hollow alumina microspheres (HAM) with the size of 50–60 μm (LLC KIT-Stroi, Russia). The sizes of alumina particles were declared by the manufacturers. From the results of BET, HAM had a specific surface area of 1.9 $m^2\ g^{-1}$ and mainly contained mesopores. Electrocorundum was revealed as a microporous material with a specific surface area of 0.1 $m^2\ g^{-1}$. X-ray diffraction analysis showed that α-Al_2O_3 was the main component in both types of raw materials. HAM also contained minor phases of γ- and θ- Al_2O_3. In the processing of porous ceramics based on electrocorundum and HAM, bentonite with a particle size of 10–30 μm originating from a Boksitogorsk mineral deposit was used as a fine technological binder. By the means of EDX, its contents were revealed as follows: Na_2O—2.83%, K_2O—1.64%, CaO—5.91%, MgO—3.43%, Al_2O_3—16.35%, SiO_2—64.23%, Fe_2O_3—5.19%, and P_2O_5—0.42%. The proportion of bentonite in its mixture with alumina fillers was in a range of 5–25 wt.%.

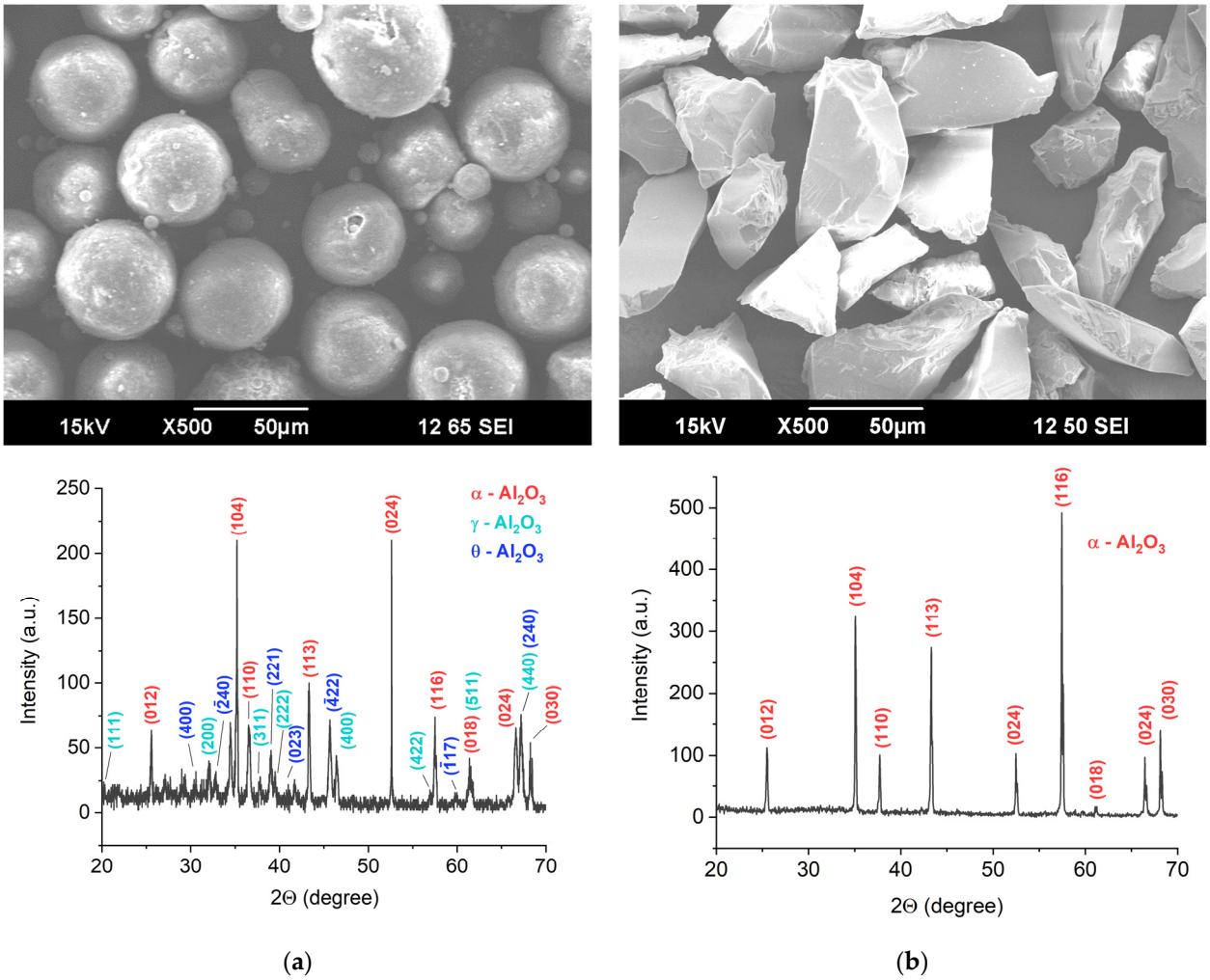

Figure 1. Morphology and phase contents of (**a**) hollow alumina microspheres and (**b**) electrocorundum F240.

2.2. Porous Ceramics Processing

2.2.1. Semi-Dry Pressing

Each type of alumina filler was proportionally mixed with bentonite. An amount of 7 wt.% of polyvinyl alcohol (PVA) (Alfa Aesar, Karlsruhe, Germany) was added to the mixture of powders. The press-powders consisting of the mentioned components were prepared by continuous mixing in a "Turbula" batch mixer (LLC Vibrotechnik, Saint-Petersburg, Russia) for 30 min. After that, the press-powders were deagglomerated by subsequent sieving through sieves with cells of 500 and 200 µm. Finally, the press-powders were stored in a closed desiccator, which was a glass container with a hermetically sealed lid, for 24 h to achieve particle wetting by PVA. The samples were uniaxially pressed at 20, 30, and 40 MPa by two-level loading and then sintered in air at 1250, 1280, 1320, and 1340 °C for 1 h.

2.2.2. Direct Casting

Preparation of ceramic samples by direct casting included preliminary mixing of the fillers (electrocorundum F240 and HAM) with bentonite binder. The content of bentonite in the mixtures reached 5–25 wt.%. The obtained mixtures were dried in air at 120 °C to constant weight, placed into a glass with melted paraffin, and kept on mixing for 20 min. The proportion of the paraffin binder in the obtained material was 25 wt.%. Then, the molding mass was placed into the EKON-UGShL (RPE EKON, Obninsk, Russia) machine and mixed in a vacuum. During the molding procedure, the temperature was maintained

at 55 °C. The samples were molded at a pressure of 40.53 kPa. Ceramics were sintered in air on a sacrificial powder at temperatures of 1280 and 1320 °C for 1 h.

2.2.3. Slip Casting

The fine fillers (electrocorundum F240 and HAM) were preliminarily mixed with 5–25 wt.% of bentonite binder. The mixtures of powders were dried to a constant weight and wetted to a humidity of 40%. After that, the mass was stabilized either by alkaline or acidic agents. The slurries based on F240 particles were stabilized by the addition of NaOH to achieve pH 12 as well as 5 wt.% of PVA as a temporary technological binder. The mixtures based on HAM possessed poor stabilization both in alkaline (pH 12) and acidic (pH 3.5) media. The samples obtained by the casting of slurries with F240 were sintered in air at 1300 °C for 1 h.

2.3. Characterization Methods

The morphology and element composition of the raw materials were studied by scanning electron microscopy (SEM) and energy-dispersive X-ray spectroscopy (EDX), respectively, by a Jeol JSM-6390 LA electron microscope (JEOL Ltd., Akishima, Tokyo, Japan). Phase analysis of the corundum fine fillers was carried out by aShimadzu XRD 6000 X-ray diffractometer (Shimadzu Corp., Kyoto, Japan) with CuKα radiation in the range of $20^\circ < 2\theta < 70^\circ$ with a step of 0.02°. XRD patterns were analyzed with Match! software (Crystal Impact GbR., Bonn, Germany) using open crystallography databases. The specific surface area of the corundum fillers was determined by the nitrogen desorption method by an Autosorb-1C/QMS automated surface analyzer (Quantachrome Inc., Boynton Beach, FL, USA). The specific surface area values were calculated by the BET method. The density and porosity of ceramic samples were obtained by the Archimedes method. To estimate the mechanical properties of ceramics, the three-point bend method was applied by an INSTRON 3382A testing machine (Instron, Norwood, MA, USA). The Microstructure of the ceramics fracture surfaces was revealed using an FEI VERSA 3D DualBeam scanning electron microscope (Thermo Fisher Scientific, Waltham, MA, USA).

3. Results

3.1. Semi-Dry Pressing

During the preparation of green bodies containing alumina filler and 5–25 wt.% of bentonite, the increase in compressing pressure from 20 to 40 MPa was accompanied by the lowering of relative porosity and the increase in the relative density of ceramics (Figures 1 and 2). The effect of sintering temperature on the density and porosity of ceramics was the most pronounced when the materials were prepared with an additional 25 wt.% of bentonite (Figures 2 and 3). However, when ceramics based on electrocorundum F240 contained this amount of the binder, it possessed lower porosity (31.3–38.6%) than similar samples produced with the addition of 5–15 wt.% of bentonite (39.1–47.5%). Ceramic discs pressed at 40 MPa possessed lower porosity than those at 20 or 30 MPa (31.3–45.1% and 33.2–47.5%, respectively). The ceramics sintered at 1250 and 1280 °C possessed insufficient transport strength.

Figure 4 shows the microstructure of ceramic samples prepared from electrocorundum F240 by sintering at 1320 °C. Bentonite in these samples is known to melt in the temperature range of 1250–1300 °C [49]. Consequently, the sintering occurred in the presence of a liquid phase. However, no traces of bentonite melt could be visualized between the particles of F240, which might be caused by its absorption by the macropores of electrocorundum. The observed microstructures were relatively homogenous with slit-and round-shaped pores of about 12 mm in diameter. The round-shaped pores were mostly present on the material pressed at 40 MPa.

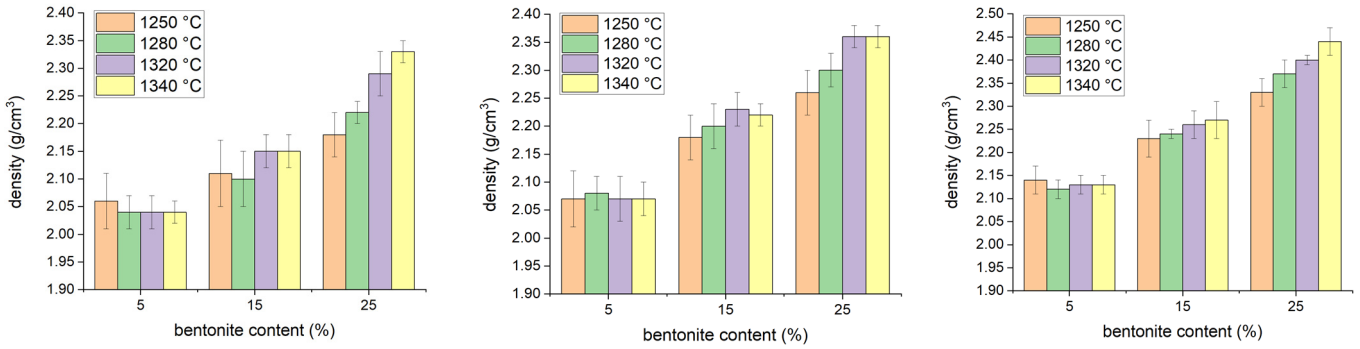

Figure 2. Content of bentonite binder vs. density of ceramics based on electrocorundum F240 pressed at (**a**) 20; (**b**) 30; and (**c**) 40 MPa. Sintering temperature is indicated in a legend.

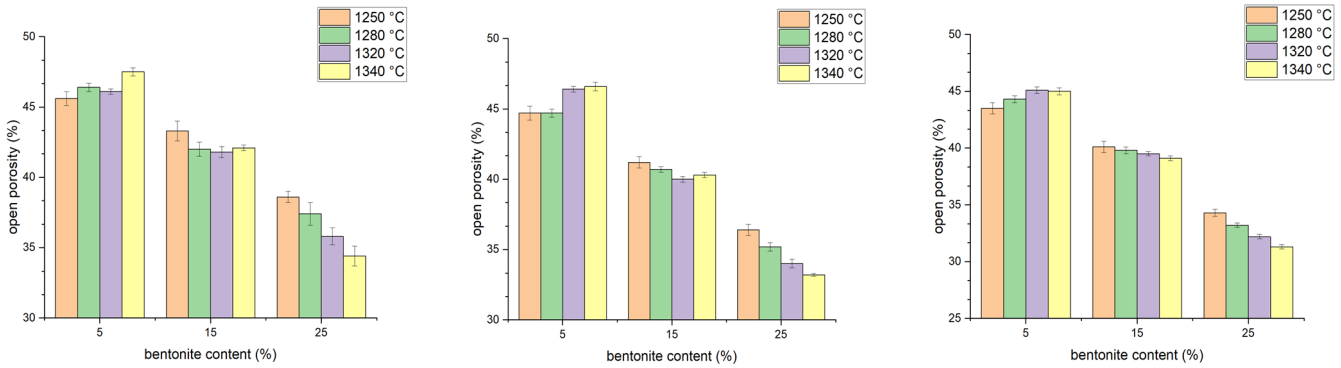

Figure 3. Content of bentonite binder vs. open porosity of ceramics based on electrocorundum F240 pressed at (**a**) 20; (**b**) 30; and (**c**) 40 MPa. Sintering temperature is indicated in a legend.

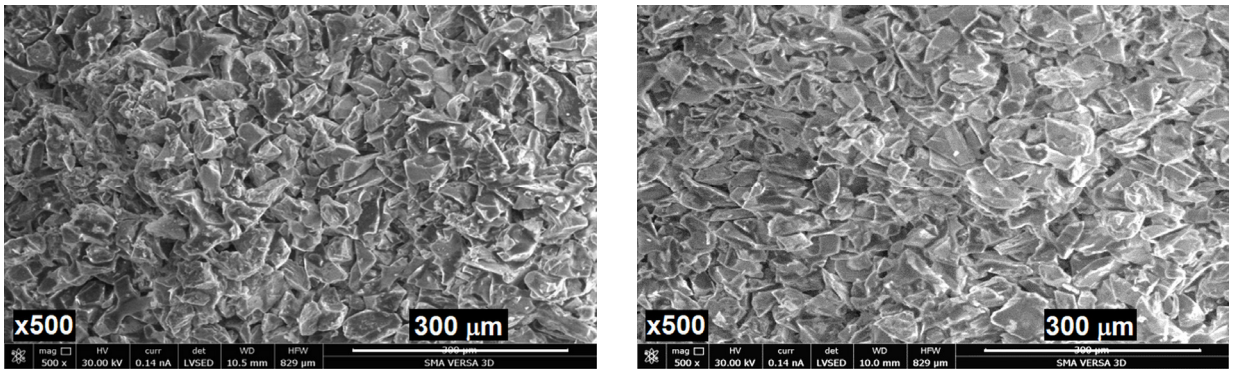

Figure 4. SEM images of fracture surfaces of ceramics based on electrocorundum F240 with 15 wt.% of bentonite binder pressed at (**a**) 30 and (**b**) 40 MPa.

The effect of bentonite content on the density and porosity of the ceramics produced with the use of HAM as a filler appeared similar to that in materials based on F240: the increase in the amount of added bentonite led to the growth in the average density and the lowering of open porosity (Figures 5 and 6). Due to the nature and structure of HAM, the increase in closed porosity, as well as the decrease in average density, were observed in these ceramics compared with those prepared from F240. A slight growth of open porosity might be related

to partial destruction of HAM during pressing. The density and porosity values demonstrated low sensitivity to the sintering temperature in a range of 1250–1340 °C.

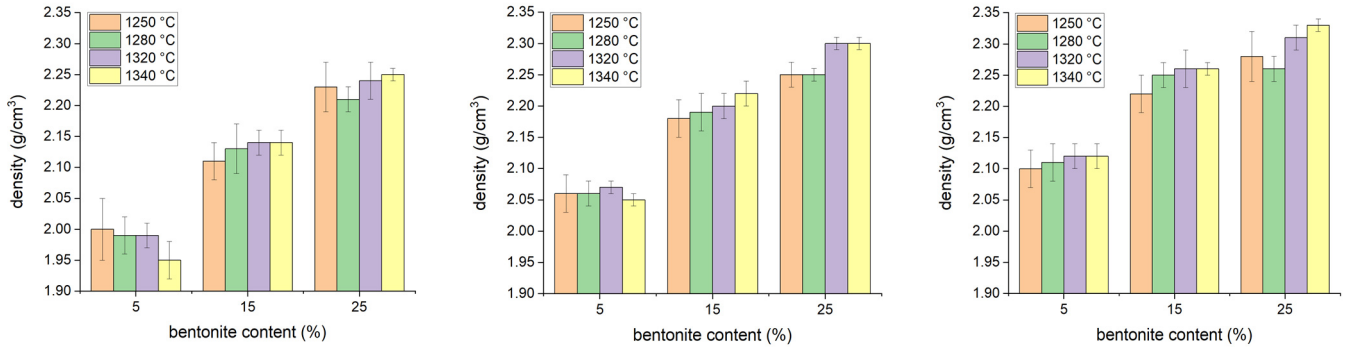

Figure 5. Content of bentonite binder vs. density of ceramics based on hollow alumina microspheres (HAM) pressed at (**a**) 20; (**b**) 30; and (**c**) 40 MPa. Sintering temperature is indicated in a legend.

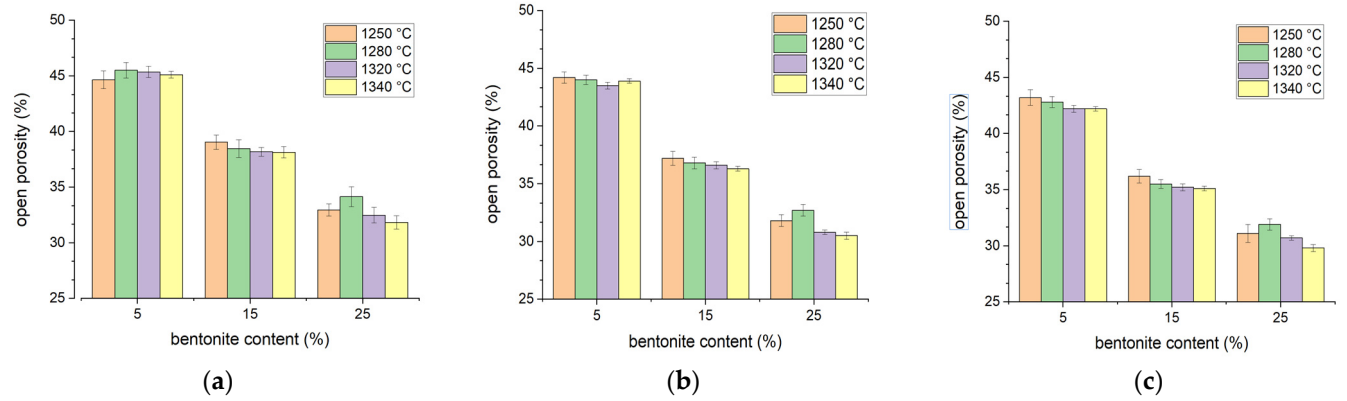

Figure 6. Content of bentonite binder vs. open porosity of ceramics based on hollow alumina microspheres (HAM) pressed at (**a**) 20; (**b**) 30; and (**c**) 40 MPa. Sintering temperature is indicated in a legend.

Liquid-phase sintering mechanism was manifested in the microstructure of ceramics prepared with HAM as a filler (Figure 7). The bentonite melt filled the space between the microspheres and formed necks there. Irregularly shaped pores of about 30–50 μm in diameter located among the microspheres more frequently appeared in the ceramics pressed at 30 MPa than at 40 MPa because of the difference in stacking and packing density of HAM.

Figure 8 demonstrates the effect of bentonite content on the flexible strength of ceramics prepared with two types of alumina fillers by pressing at 30 MPa and subsequent sintering at 1300 °C. The samples consisting of 5 wt.% of bentonite binder possessed comparatively low flexible strength (5.2–22.3 MPa). When the bentonite additive reached 15–25 wt.%, the gradual growth in the strength of both types of material was observed (to 58.1–67.4 MPa for ceramics with F240; to 37.8–51.6 MPa for HAM-containing material). This strengthening was attributed to the reduction in porosity. The ceramics produced from electrocorundum had higher flexible strength than the materials prepared with the use of microspheres. The reported elastic modulus of alumina ceramics is about 400 GPa, while this value does not exceed 100 GPa for the binder [50–52]. For this reason, the propagation of cracks in the studied materials mostly occurred at the periphery of the filler particles, through bentonite [53]. Contact points of neighboring microspheres and the necks between them were much smaller than pores and could serve as the places for the formation of critical cracks [54]. Due to the irregular shape, the particles of electrocorundum formed numerous contacts as well as effectively blocked the crack propagation. The flexible strength

of ceramics with equal amounts of bentonite also appeared to be affected by the porosity, which was slightly higher in the material with HAM.

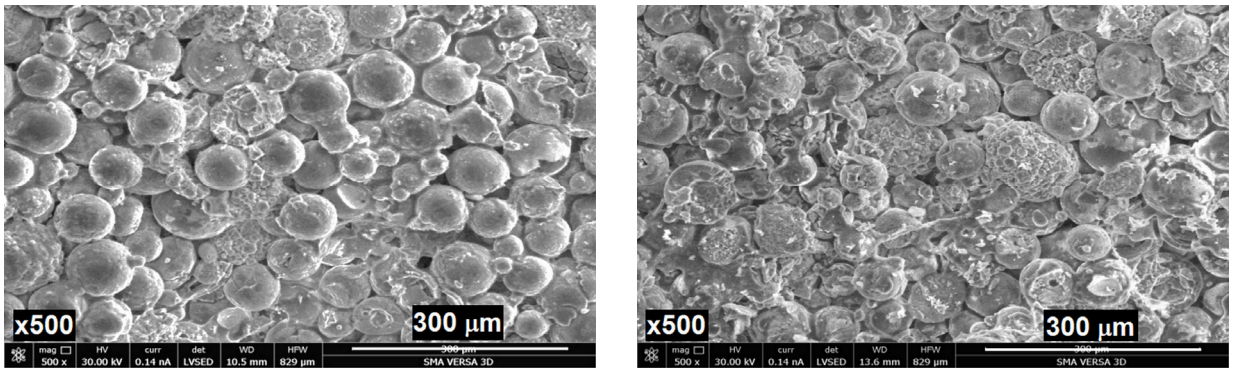

(**a**) (**b**)

Figure 7. SEM images of fracture surfaces of ceramics based on hollow alumina microspheres (HAM) with 15 wt.% of bentonite binder pressed at (**a**) 30 and (**b**) 40 MPa.

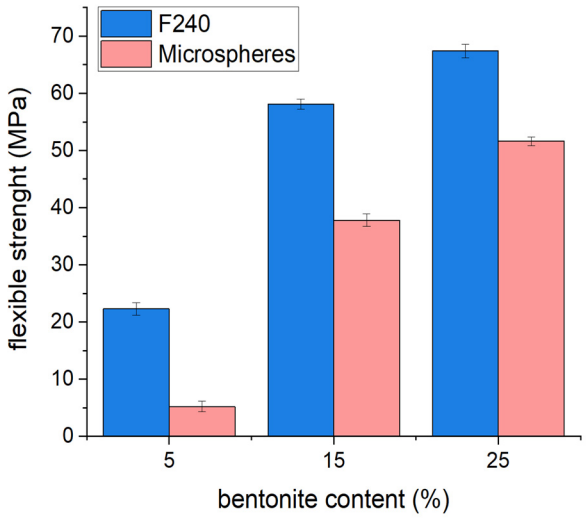

Figure 8. Flexible strength of ceramics produced with electrocorundum F240 of hollow alumina microspheres as fillers vs. bentonite binder content in them.

3.2. Direct Casting

The samples of alumina ceramics prepared by direct casting method with the addition of 5 wt.% of bentonite and subsequently sintered at 1320 °C showed low density and high open porosity (44.7–46.8%) (Figure 9). These properties were accompanied by poor transport strength because the amount of bentonite binder they contained appeared to be not enough to cover the alumina particles and provide their sintering. The transport strength was raised when the bentonite content was increased to 15–25 wt.%. At the same time, a gradual lowering in porosity was observed for electrocorundum-based materials (to 42.3–40.1%) as well as for HAS-based ceramics (to 44.3–41.2%).

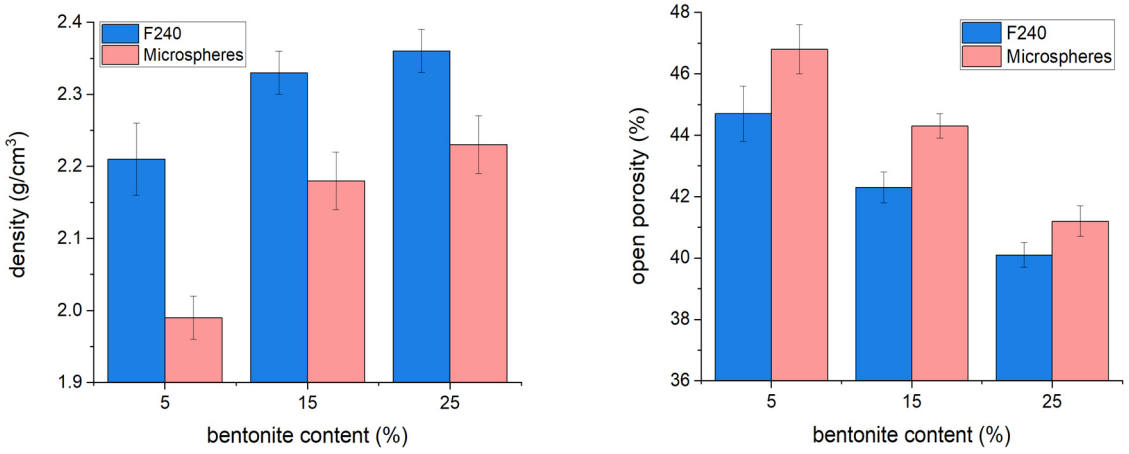

(**a**) (**b**)

Figure 9. (**a**) Density and (**b**) open porosity of alumina ceramics based on electrocorundum F240 and hollow alumina microspheres produced by direct casting with different amounts of bentonite binder.

The microstructure ceramics manufactured by direct casting from electrocorundum was not sensitive to the sintering temperature (Figure 10a,b). After sintering at 1280 as well as at 1320 °C, the filler particles were homogenously arranged in the bulk and separated by the pores with elongated shapes and sizes of 15–90 µm.

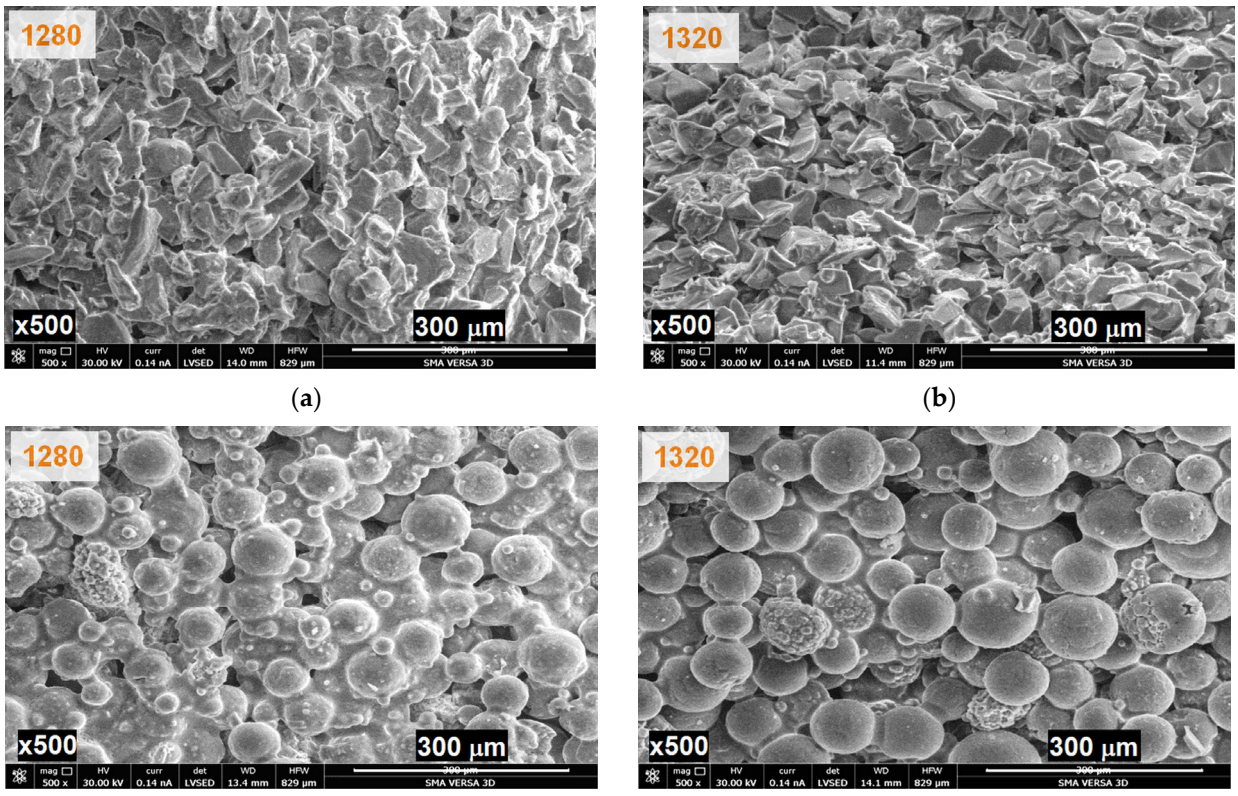

(**a**) (**b**)

(**c**) (**d**)

Figure 10. SEM images of fracture surfaces of ceramics based on (**a**,**c**) electrocorundum F240 and (**b**,**d**) hollow alumina microspheres prepared with 15 wt.% of bentonite binder by direct casting. The figures indicate the sintering temperature in °C.

With the temperature raise from 1280 to 1320 °C, the melting of bentonite was nearing completion. This resulted in the wetting of hollow microspheres, the formation of numerous

necks between them, and an increase in the number of their contacts (Figure 10c,d). The pore size was not dependent on the sintering temperature and reached 30–100 μm, exceeding the corresponding value for the materials with F240 as a filler.

An amount of 5 wt.% of bentonite appeared insufficient to obtain flex-resistant alumina ceramics both with F240 and HAM fillers (Figure 11). Similar to ceramics prepared by semi-dry pressing, the increase in bentonite proportion to 15 and 25 wt.% resulted in a significant increase in ceramics' flexible strength: up to 65.5 MPa in the case of F240 and 45.8 MPa in the ceramics with HAM. Electrocorundum-based materials were stronger for bending than materials containing microspheres. However, alumina ceramics prepared by direct casting possessed 5–8 MPa lower strength than the pressed materials.

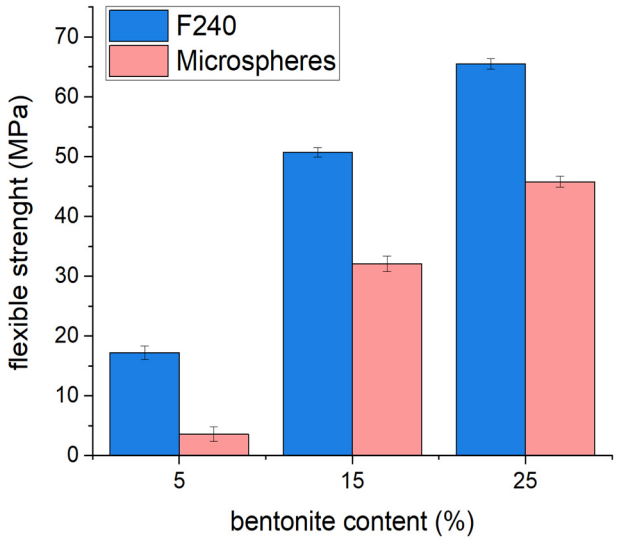

Figure 11. Flexible strength of ceramics produced with electrocorundum F240 of hollow alumina microspheres as fillers vs. bentonite binder content in them. Direct casting, sintering at 1300 °C.

3.3. Slip Casting

Figure 12 shows the integral structural and mechanical properties of the ceramics manufactured from electrocorundum F240 by slip casting. The average density of these materials was significantly lower than for the related ceramics produced by semi-dry pressing or direct casting. Even with the addition of 25 wt.% of bentonite, the density not exceeded 2.05 g cm^{-3}. In the case of semi-dry pressing as well as direct casting, close values were obtained when the ceramics were processed with 5 wt.% of the binder. The porosity of slip-casted ceramics dropped from 50 to 45% with the amount of bentonite increasing from 5 to 25 wt.%. This was accompanied by the increase in their flexible strength from 21 to 45 MPa (Figure 12c), which could be explained by the changes in the microstructure. These changes include the reduction in pore sizes and the homogenous distribution of bentonite between the particles of F240 (Figure 13).

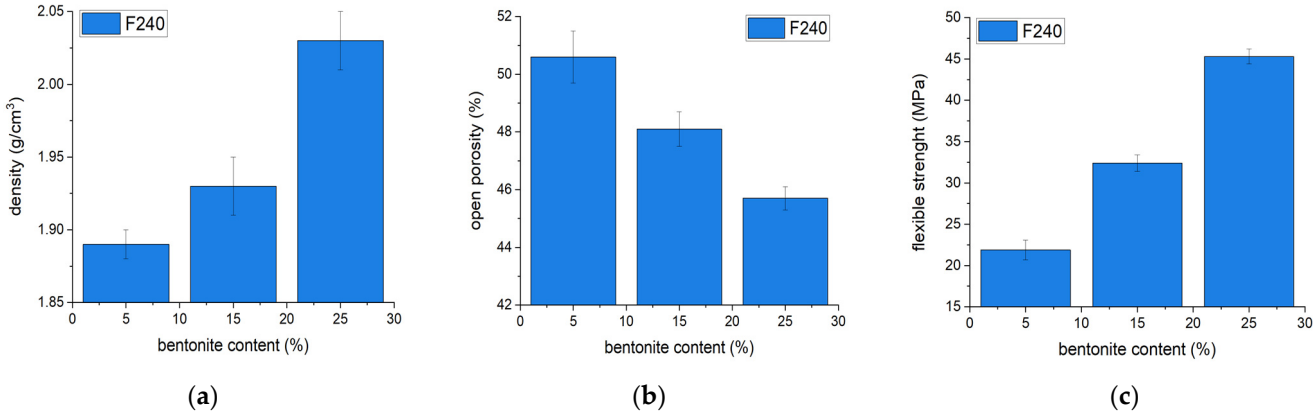

Figure 12. Content of bentonite binder vs. (**a**) density, (**b**) open porosity, and (**c**) flexible strength of ceramics based on electrocorundum F240 prepared by slip casting.

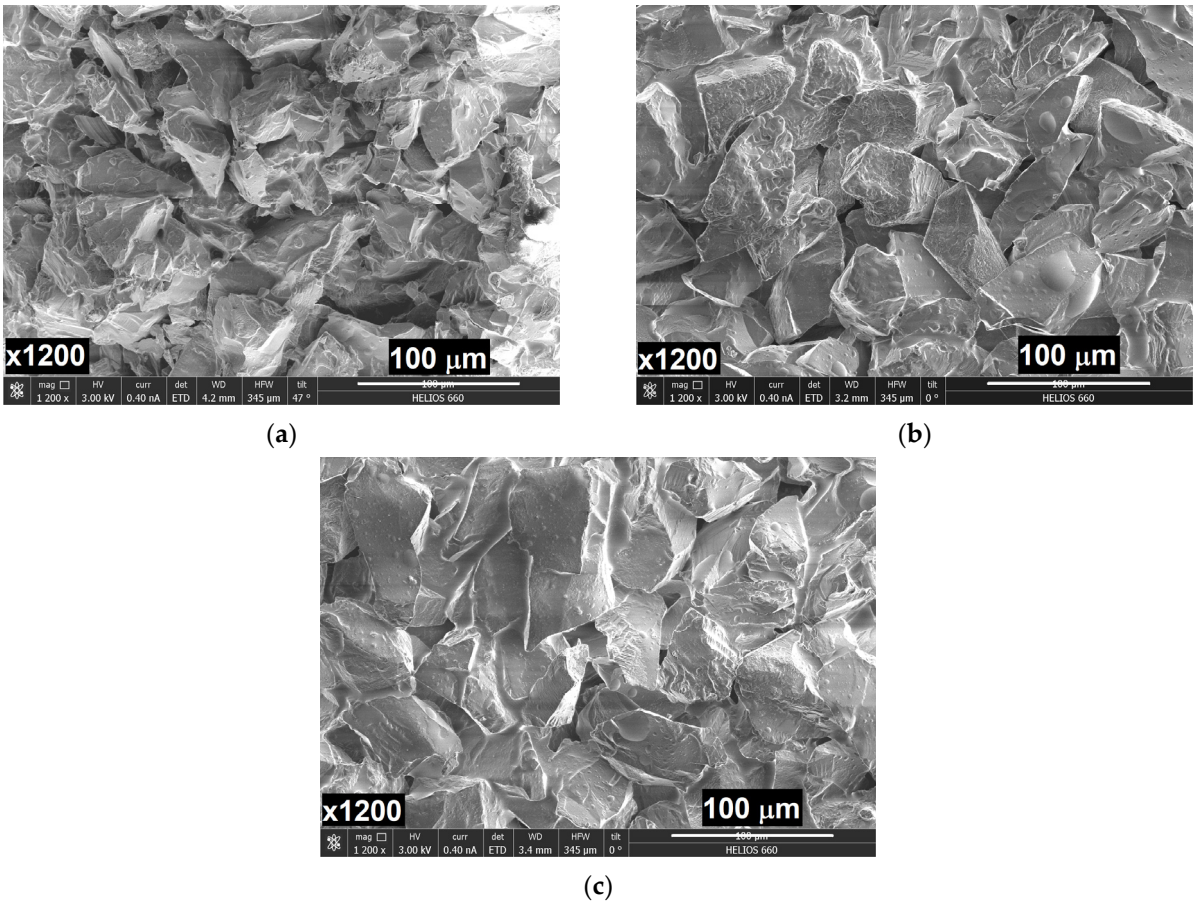

Figure 13. SEM images of fracture surfaces of ceramics based on electrocorundum F240 and obtained by slip casting with (**a**) 5, (**b**) 15, and (**c**) 20 wt.% of bentonite binder. The figures indicated the sintering temperature in °C.

4. Discussion

Pressing and casting techniques yielded alumina ceramics with a wide range of pore sizes and different shapes of pores (Table 1). In most cases, the increase in porosity led to the deterioration of mechanical properties. The results from this study confirmed this pattern. Due to the selection of the required amount of binder, the produced ceramics possessed moderate porosity but increased flexible strength compared with that of other reported results. It was found that for the shaping techniques in which pressure is applied, the

addition of 5 wt.% bentonite binder is not enough to achieve sufficient transport strength of the green bodies. When the content of bentonite was 25 wt.%, an excess amount of its melt, which formed during the sintering, led to undesirable compaction and closure of pores. Thus, both when using electrocorundum and alumina microspheres as the fillers, about 15 wt.% of bentonite is required to obtain strong porous ceramics. The preferred sintering temperature for the studied compositions is about 1300 °C.

Table 1. Properties of porous alumina ceramics produced by pressing and casting techniques with different binders.

Molding Technique	Filler	Binder	Porosity (%)	Pore Size (μm)	Tensile Strength (MPa)	Flexible Strength (MPa)	Reference
Pressing	Electrocorundum	Porcelain	17–26	1.2–4.1	n/a	0.5–15.1	[44]
	Electrocorundum	Porcelain	44	n/a *	n/a	14.6	[45]
	Corundum	Rice husk, sugar cane cake	44–67	70–178	1.5–20.4	n/a	[13]
	Corundum	Kyanite, white clay	42	248.8	n/a	n/a	[10]
	Corundum	Quartz, calcite, microcline	66.1	1.32	n/a	23.8	[7]
	Electrocorundum	Bentonite	40.0–40.7	n/a	n/a	58.1	this study
	HAM **	$CaSiO_3$, Na_2SiO_3	78–81	n/a	n/a	n/a	[31]
	HAM	SiO_2	61.9	n/a	n/a	n/a	[34]
	HAM	Bentonite	36.6–36.8	n/a	n/a	37.8	this study
Gel casting	Corundum	mCaO·$n$$Al_2O_3$	76–83	1–1700	n/a	n/a	[24]
	Corundum	Kaolinite	45.0–47.9	1.28–2.55	n/a	n/a	[23]
Slip casting	Corundum	mCaO·$n$$Al_2O_3$	73.7	348	n/a	n/a	[18]
	α+γ Al_2O_3	SiO_2	56–64	~1–1000	n/a	3.2–11.0	[20]
	Electrocorundum	Bentonite	48.1	n/a	n/a	32.4	this study
Direct casting	HAM	Bentonite	44.3	n/a	n/a	32.1	this study
	Electrocorundum	Bentonite	42.3	n/a	n/aa	50.7	this study

* n/a—not available; ** HAM—hollow alumina microspheres.

Compared with the pressing techniques, in wet forming methods, an increase in the porosity is observed due to the free stacking of particles from the slurry during the liquid component removal. From the results obtained for ceramics with electrocorundum filler, the highest porosity could be achieved with the use of the slip-casting technique. The slurries in the direct casting and slip casting methods were prepared with different liquid components: in the first case, with paraffin; in another, it was water-based. Previously, in the manufacture of dense ceramics, it was described how the removal of temporary binders upon heating could depend on the binder's nature [55]. The burnout of residual paraffin was preceded by its partial melting (about 50 °C) and leakage from the green body, inside which the capillary forces arose, constricting the pores. In the case of slip casting, the water contained in the green body evaporated upon heating without any similar effects on the pores.

Stabilization of the slip by adding electrolytes, such as acids or bases, is caused by the change in the electric potential on the particles' surface due to ion exchange. This study required the approach and aggregation of particles to increase with the electric potential, resulting in aggregative stability of the suspension [56]. The fillers used in this study had different phase compositions and surface acidity. Unlike electrocorundum (α-Al_2O_3), the microspheres contained other aluminum oxide modifications, in particular, γ-Al_2O_3. The latter has the structure of a defective spinel, due to which strong acid Lewis centers are presented on its surface [57]. The inherent acidity of γ-Al_2O_3 complicated the search for the composition of the electrolyte to stabilize the slip. However, inhomogeneous phase content is typical for HAM because of their production technique [58,59].

The results obtained in this study showed that the use of wet forming methods is beneficial for the porosity of ceramics with alumina fillers, and at the same time leads to a decrease in the mechanical strength of the material compared with that of semi-dry pressing. In the manufacture of ceramics based on microspheres, the direct casting method is of particular interest. It is customary for some authors to divide pores in ceramics containing microspheres into two types: α—intrinsic internal pores of microspheres and β—pores formed between the microspheres [31,32]. The use of direct casting in combination with a

low amount of bentonite allowed the preservation of α-porosity compared with pressing, since during casting, the microspheres are not subjected to the applied pressure. In addition, direct casting, in contrast to slip casting, does not involve the stage of selecting a stabilizer for the slip with a specific filler.

5. Conclusions

(a) The detailed study of microstructure, integral structural, and mechanical properties of porous alumina ceramics with two different types of filler was performed for the materials prepared by pressing (semi-dry pressing) and casting (direct casting, slip casting) techniques.
(b) The use of semi-dry pressing allowed us to obtain high flexural strength in porous alumina ceramics (up to 58 MPa with elecrocorumdum F240 as a filler). Meanwhile, casting techniques provided high values of porosity (up to 48% in the case of slip casting with electrocorundum F240).
(c) Independent from the shaping technique, the ceramics containing hollow microspheres were inferior to those with electrocorundum F240 in terms of flexural strength but possessed close values of porosity.
(d) The direct casting method was revealed to fit well for the production of porous ceramics with hollow alumina microspheres as a filler as it maintained the integrity of the filler particles and thus provided higher porosity compared with that of the pressing technique.

Author Contributions: Conceptualization, A.D.S., V.V.R. and V.P.T.; methodology, A.D.S.; formal analysis, A.D.S. and A.A.K.; investigation, A.D.S.; resources, A.D.S., V.V.R. and V.P.T.; data curation, A.D.S.; writing—original draft preparation, A.D.S. and A.A.K.; writing—review and editing, A.D.S. and A.A.K.; visualization, A.D.S. and A.A.K. All authors have read and agreed to the published version of the manuscript.

Funding: This research received no external funding.

Institutional Review Board Statement: Not applicable.

Informed Consent Statement: Not applicable.

Data Availability Statement: The data presented in this study are available on request from the corresponding author after obtaining the permission of an authorized person.

Acknowledgments: This work was supported in part by the Lomonosov Moscow State University Program of development.

Conflicts of Interest: The authors declare no conflict of interest.

References

1. Liu, P.; Chen, G.-F. Applications of porous ceramics. In *Porous Materials Processing and Applications*, 1st ed.; Elsevier Inc.: Amsterdam, The Netherlands, 2014; pp. 303–344. [CrossRef]
2. Sarkar, N.; Kim, I.J. Porous Ceramics. In *Advanced Ceramic Processing*; Mohamed, A., Ed.; IntechOpen: London, UK, 2015; pp. 55–84. [CrossRef]
3. Krasnyi, B.L.; Tarasovskii, V.P.; Mosin, Y.M.; Krasnyi, A.B.; Omarov, A.Y. Porous permeable corundum ceramics formed out of aluminum hydroxide powders. Part I. The investigation of aluminum hydroxide powders of various brands. *Novye Ogneup. New Refract.* **2014**, *1*, 35–41. (In Russian)
4. Xu, G.; Ma, Y.; Cui, H.; Ruan, G.; Zhang, Z.; Zhao, H. Preparation of porous mullite-corundum ceramics with controlled pore size using bioactive yeast as pore-forming agent. *Mater. Lett.* **2014**, *116*, 349–352. [CrossRef]
5. Kiwerski, J.E.; Ogonowski, A.; Bieniek, J.; Krasuski, M. The use of porous corundum ceramics in spinal surgery. *Int. Orthop.* **1994**, *18*, 10–13. [CrossRef]
6. Grigoriev, M.V.; Burlachenko, A.G.; Buyakova, S.P.; Kul'kov, S.N. Deformation and Fracture of Corundum Ceramics with a Multilevel Pore Structure. *Tech. Phys.* **2019**, *64*, 1803–1807. [CrossRef]
7. Hua, K.; Shui, A.; Xu, L.; Zhao, K.; Zhou, Q.; Xi, X. Fabrication and characterization of anorthite-mullite-corundum porous ceramics from construction waste. *Ceram. Int.* **2016**, *42*, 6080–6087. [CrossRef]

8. Miao, Z.; Li, N.; Yan, W. Effect of sintering temperature on the phase composition and microstructure of anorthite-mullite-corundum porous ceramics. *Ceram. Int.* **2014**, *40*, 15795–15799. [CrossRef]
9. Xiong, X.; Wang, Z.; Wang, X.; Liu, H.; Ma, Y. Enhancing the mechanical strength and air permeability of corundum porous materials using shape-modified coarse aggregates. *Ceram. Int.* **2019**, *45*, 11027–11031. [CrossRef]
10. Zhang, Z.; Yan, W.; Li, N.; Li, Y.; Zhou, W.; Han, B. Influence of spherical porous aggregate content on microstructures and properties of gas-permeable mullite-corundum refractories. *Ceram. Int.* **2019**, *45*, 17268–17275. [CrossRef]
11. Zhao, F.; Ge, T.; Gao, J.; Chen, L.; Liu, X. Transient liquid phase diffusion process for porous mullite ceramics with excellent mechanical properties. *Ceram. Int.* **2018**, *44*, 19123–19130. [CrossRef]
12. Zhou, W.; Yan, W.; Li, N.; Li, Y.; Dai, Y.; Zhang, Z.; Ma, S. Fabrication of mullite-corundum foamed ceramics for thermal insulation and effect of micro-pore-foaming agent on their properties. *J. Alloys Compd.* **2019**, *785*, 1030–1037. [CrossRef]
13. Dele-Afolabi, T.T.; Hanim, M.A.A.; Norkhairunnisa, M.; Sobri, S.; Calin, R. Investigating the effect of porosity level and pore former type on the mechanical and corrosion resistance properties of agro-waste shaped porous alumina ceramics. *Ceram. Int.* **2017**, *43*, 8743–8754. [CrossRef]
14. Wang, S.; Yang, Z.; Luo, X.; Qi, X.; Zhang, L.; You, J. Preparation of calcium hexaluminate porous ceramics by gel-casting method with polymethyl methacrylate as pore-forming agent. *Ceram. Int.* **2022**, *48*, 30356–30366. [CrossRef]
15. Meng, X.; Xu, J.; Yang, R.; Wei, R.; Zhu, J.; Yang, J.; Gao, F. Lanthanum zirconate porous ceramics with controllable secondary pores for high-temperature thermal insulation. *Ceram. Int.* **2022**, *48*, 33976–33983. [CrossRef]
16. Sooksaen, P.; Karawatthanaworrakul, S. The properties of Southern Thailand clay-based porous ceramics fabricated from different pore size templates. *Appl. Clay Sci.* **2015**, *104*, 295–302. [CrossRef]
17. Wu, Q.; Huang, Z. Preparation and performance of lightweight porous ceramics using metallurgical steel slag. *Ceram. Int.* **2021**, *47*, 25169–25176. [CrossRef]
18. Zhou, W.; Yan, W.; Li, N.; Li, Y.; Dai, Y.; Zhang, Z. Effect of microsilica content on microstructure and properties of foamed ceramics with needle-like mullite. *Process. Appl. Ceram.* **2019**, *13*, 202–209. [CrossRef]
19. Li, S.; Li, N. Influences of composition of starting powders and sintering temperature on the pore size distribution of porous corundum-mullite ceramics. *Sci. Sinter.* **2005**, *37*, 173–180. [CrossRef]
20. Zake-Tiluga, I.; Svinka, R.; Svinka, V. Highly porous corundum-mullite ceramics—Structure and properties. *Ceram. Int.* **2014**, *40*, 3071–3077. [CrossRef]
21. Li, X.; Li, S.; Yin, Z.; Shi, W.; Tao, M.; Liu, W.; Gao, Z.; Ma, C. Foam-gelcasting preparation and properties of high-strength mullite porous ceramics. *Ceram. Int.* 2022; *in press*. [CrossRef]
22. Li, X.; Yan, L.; Gou, A.; Du, H.; Huo, F.; Liu, J. Lightweight porous silica-alumina ceramics with ultra-low thermal conductivity. *Ceram. Int.* 2022; *in press*. [CrossRef]
23. Liu, Y.F.; Liu, X.Q.; Li, G.; Meng, G.Y. Low cost porous mullite-corundum ceramics by gelcasting. *J. Mater. Sci.* **2001**, *36*, 3687–3692. [CrossRef]
24. Zhang, Z.; Zhou, W.; Han, B.; Li, Y.; Yan, W.; Xu, N.; Li, N.; Wei, J. Preparation and characterization of eco-friendly and low-cost mullite-corundum foamed ceramics with low thermal conductivity. *Ceram. Int.* **2019**, *45*, 13203–13209. [CrossRef]
25. Zhang, X.; He, J.; Han, L.; Huang, Z.; Xu, K.; Cai, W.; Wu, S.; Jia, Q.; Zhang, H.; Zhang, S. Foam gel-casting preparation of SiC bonded ZrB2 porous ceramics for high-performance thermal insulation. *J. Eur. Ceram. Soc.* **2023**, *43*, 37–46. [CrossRef]
26. Dong, X.; Chua, B.W.; Li, T.; Zhai, W. Multi-directional freeze casting of porous ceramics with bone-inspired microstructure. *Mater. Des.* **2022**, *224*, 111344. [CrossRef]
27. Li, L.; Li, X.; Dong, X.; Zhang, Q.; Yan, L.; Liu, J.; Guo, A. Hierarchically porous Al_2TiO_5 ceramics via freeze-gel casting. *Ceram. Int.* **2022**, *48*, 22343–22351. [CrossRef]
28. Liu, P.S.; Chen, G.F. Fabricating porous ceramics. In *Porous Materials*, 1st ed.; Elsevier Inc.: Amsterdam, The Netherlands, 2014; pp. 221–302. [CrossRef]
29. Zhang, Y.; Yao, D.; Zuo, K.; Xia, Y.; Yin, J.; Liang, H.; Zeng, Y.-P. Self-propagating high temperature synthesis (SHS) of porous Si_3N_4-based ceramics with considerable dimensions and study on mechanical properties and oxidation behavior. *J. Eur. Ceram. Soc.* **2021**, *41*, 4452–4461. [CrossRef]
30. Zhang, Y.; Yao, D.; Zuo, K.; Xia, Y.; Yin, J.; Liang, H.; Zeng, Y.-P. The synthesis of single-phase β-Sialon porous ceramics using self-propagating high-temperature processing. *Ceram. Int.* **2022**, *48*, 4371–4375. [CrossRef]
31. Yang, J.L.; Xu, X.X.; Wu, J.M.; Wang, X.H.; Su, Z.G.; Li, C.H. Preparation of Al_2O_3 poly-hollow microsphere (PHM) ceramics using Al_2O_3 PHMs coated with sintering additive via co-precipitation method. *J. Eur. Ceram. Soc.* **2015**, *35*, 2593–2598. [CrossRef]
32. Qi, F.; Xu, X.; Xu, J.; Wang, Y.; Yang, J. A Novel Way to Prepare Hollow Sphere Ceramics. *J. Am. Ceram. Soc.* **2014**, *97*, 3341–3347. [CrossRef]
33. Su, Z.; Xi, X.; Hu, Y.; Fei, Q.; Yu, S.; Li, H.; Yang, J. A new Al_2O_3 porous ceramic prepared by addition of hollow spheres. *J. Porous Mater.* **2014**, *21*, 601–609. [CrossRef]
34. Geng, H.; Hu, X.; Zhou, J.; Xu, X.; Wang, M.; Guo, A.; Du, H.; Liu, J. Fabrication and compressive properties of closed-cell alumina ceramics by binding hollow alumina spheres with high-temperature binder. *Ceram. Int.* **2016**, *42*, 16071–16076. [CrossRef]
35. Mummareddy, B.; Burden, E.; Carrillo, J.G.; Myers, K.; MacDonald, E.; Cortes, P. Mechanical performance of lightweight ceramic structures via binder jetting of microspheres. *SN Appl. Sci.* **2021**, *3*, 402. [CrossRef]

36. Xia, B.; Wang, Z.; Gou, L.; Zhang, M.; Guo, M. Porous mullite ceramics with enhanced compressive strength from fly ash-based ceramic microspheres: Facile synthesis, structure, and performance. *Ceram. Int.* **2022**, *48*, 10472–10479. [CrossRef]
37. Vakalova, T.V.; Revva, I.B. Highly porous building ceramics based on «clay-ash microspheres» and «zeolite-ash microspheres» mixtures. *J. Con. Build. Mat.* **2022**, *317*, 125922. [CrossRef]
38. Yan, W.; Chen, Q.; Lin, X.; Li, N. Pore characteristics and phase compositions of porous corundum-mullite ceramics prepared from kaolinite gangue and $Al(OH)_3$ with different amount of $CaCO_3$ addition. *J. Ceram. Soc. Jpn.* **2015**, *123*, 897–902. [CrossRef]
39. Yang, M.; Li, J.; Man, Y.; Peng, Z.; Zhang, X.; Luo, X. A novel hollow alumina sphere-based ceramic bonded by in situ mullite whisker framework. *Mater. Des.* **2020**, *186*, 108334. [CrossRef]
40. Mahnicka, L.; Svinka, R.; Svinka, V. Influence of kaolin and firing temperature on the mullite formation in porous mullite-corudum materials. In Proceedings of the IOP Conference Series: Materials Science and Engineering, Riga, Latvija, 23–25 May 2011. [CrossRef]
41. Zhang, F.; Li, Z.; Xu, M.; Wang, S.; Yang, J. A review of 3D printed porous ceramics. *J. Eur. Ceram. Soc.* **2022**, *42*, 3351–3373. [CrossRef]
42. Medvedovski, E.; Peltsman, M. Low pressure injection moulding mass production technology of complex shape advanced ceramic components. *Adv. Appl. Ceram.* **2012**, *111*, 333–344. [CrossRef]
43. Krasnyi, B.L.; Tarasovskii, V.P.; Krasnyi, A.B.; Uss, A.M. Effect of electromelted corundum crystal size and shape on the microstructure and permeability of porous ceramic. *Refract. Ind. Ceram.* **2009**, *50*, 451–455. [CrossRef]
44. Belyakov, A.V.; Oo, Z.Y.M.; Popova, N.A.; Min, Y.A. Effect of Electrocorundum Powder Grain Size Composition with a Porcelain Binder on Porous Ceramic Gas Permeability and Strength. *Refract. Ind. Ceram.* **2017**, *58*, 390–394. [CrossRef]
45. Belyakov, A.V.; Oo, Z.Y.M.; Popova, N.A.; Min, Y.A. Permeable ceramic filled with trifractional electrofused corundum and porcelain bond. *Novye Ogneup. (New Refract.)* **2018**, *8*, 24–27. (In Russian) [CrossRef]
46. Tarasovskii, V.P.; Krasnyi, B.L.; Koshkin, V.I.; Borovin, Y.M.; Vasin, A.A.; Smirnov, A.D.; Kudryash, M.N. Quantitative analysis of the structure of permeable ceramics made from a powder of narrowfractionated electrocorundum and hollow corundum microspheres. *Novye Ogneup. New Refract.* **2016**, *6*, 49–52. (In Russian)
47. Krasnyi, B.L.; Tarasovskii, V.P.; Koshkin, V.I.; Vasin, A.A.; Kormilitsin, M.N.; Novoselov, R.A.; Smirnov, A.D. Quantitative analysis of the structure of permeable ceramics from narrowfractionated electrocorundum powders of various dispersions. *Novye Ogneup. New Refract.* **2015**, *11*, 58–62. (In Russian)
48. Szafran, M.; Wiśniewski, P. Effect of the bonding ceramic material on the size of pores in porous ceramic materials. *Colloids Surfaces A Physicochem. Eng. Asp.* **2001**, *179*, 201–208. [CrossRef]
49. Rao, P.N. *Manufacturing Technology: Foundry, Forming, and Welding*, 2nd ed.; Hill Publishing Company Ltd.: New Delhi, India, 1998; pp. 193–200.
50. Wan, D.; Bao, Y.; Liu, X.; Zhao, H.; Tian, L. Evaluation of elastic modulus and strength of glass and brittle ceramic materials by compressing a notched ring specimen. *Adv. Mater. Res.* **2010**, *177*, 114–117. [CrossRef]
51. Fu, L.; Engqvist, H.; Xia, W. Glass-ceramics in dentistry: A review. *Materials* **2020**, *13*, 1049. [CrossRef]
52. Bogdanov, S.P.; Kozlov, V.V.; Shevchik, A.P.; Dolgin, A.S. Young's Modulus of Corundum Ceramics Sintered from Powders with a Core-Shell Structure Synthesized by Iodine Transport. *Refract. Ind. Ceram.* **2019**, *60*, 405–408. [CrossRef]
53. Richerson, D.W. *Modern Ceramic Egineering: Properties, Processing and Use in Design*, 3rd ed.; CRC Press: Boca Raton, FL, USA; Taylor & Francis Group: New York, NY, USA, 2006; pp. 235–268.
54. Lee, W.D.; Rainforth, W.M. *Ceramic Microstructures: Property Control by Processing*, 1st ed.; Chapman & Hall: London, UK, 1994; pp. 110–111.
55. Kholodkova, A.A.; Danchevskaya, M.N.; Ivakin, Y.D.; Muravieva, G.P.; Smirnov, A.D.; Tarasovskii, V.P.; Ponomarev, S.G.; Fionov, A.S.; Kolesov, V.V. Properties of barium titanate ceramics based on powder synthesized in supercritical water. *Ceram. Int.* **2018**, *44*, 13129–13138. [CrossRef]
56. Klimosh, Y.A.; Levitskii, I.A. Rheological properties of slips based on polymineral clays with the addition of electrolytes. *Glass Ceram.* **2004**, *61*, 375–378. [CrossRef]
57. Fierro, J.L.G. (Ed.) *Metal Oxides: Chemistry and Applications*; Taylor & Francis Gruop, LLC: Boca-Raton, FL, USA, 2006.
58. Károly, Z.; Szépvölgyi, J. Hollow alumina microspheres prepared by RF thermal plasma. *Powder Technol.* **2003**, *132*, 211–215. [CrossRef]
59. Hu, Y.; Li, C.; Gu, F.; Ma, J. Preparation and formation mechanism of alumina hollow nanospheres via high-speed jet flame combustion. *Ind. Eng. Chem. Res.* **2007**, *46*, 8004–8008. [CrossRef]